Human Molecular Genetics, 2000, Vol. 9, No. 7 **1075–1085**

Characterization of the sialidase molecular defects in sialidosis patients suggests the structural organization of the lysosomal multienzyme complex

Kiven E. Lukong, Marc-André Elsliger+, Yuan Chang, Catherine Richard, George Thomas[1], William Carey[2], Anna Tylki-Szymanska[3], Barbara Czartoryska[4], Tina Buchholz[5], German Rodríguez Criado[6], Silvia Palmeri[7] and Alexey V. Pshezhetsky§

Service de Génétique Médicale, Hôpital Sainte-Justine, 3175 Côte Ste-Catherine and Département de Pédiatrie, Faculté de Médicine, Université de Montréal, Montréal, Quebec H3T 1C5, Canada, [1]John Hopkins University School of Medicine, USA, [2]Women's and Children's Hospital, North Adelaide, Australia, [3]Metabolic Diseases Department, Child Health Center, Warsaw, Poland, [4]Institute of Psychiatry and Neurology, Warsaw, Poland, [5]Klinikum Grosshadern, Munich, Germany, [6]Unidad de Dismorfología, Hospital Virgen del Rocío, Sevilla, Spain and [7]Institute of Neurological Sciences, University of Siena, Italy

Received 22 November 1999; Revised and Accepted 28 January 2000

Sialidosis is an autosomal recessive disease caused by the genetic deficiency of lysosomal sialidase, which catalyzes the hydrolysis of sialoglycoconjugates. The disease is associated with progressive impaired vision, macular cherry-red spots and myoclonus (sialidosis type I) or with skeletal dysplasia, Hurler-like phenotype, dysostosis multiplex, mental retardation and hepatosplenomegaly (sialidosis type II). We have analyzed the genomic DNA from nine sialidosis patients of multiple ethnic origin in order to find mutations responsible for the enzyme deficiency. The activity of the identified variants was studied by transgenic expression. One patient had a frameshift mutation (G623delG deletion), which introduced a stop codon, truncating 113 amino acids. All others had missense mutations: G679G→A (Gly227Arg), C893C→T (Ala298Val), G203G→T (Gly68Val), A544A→G (Ser182Gly) C808C→T (Leu270Phe) and G982G→A (Gly328Ser). We have modeled the three-dimensional structure of sialidase based on the atomic coordinates of the homologous bacterial sialidases, located the positions of mutations and estimated their potential effect. This analysis showed that five mutations are clustered in one region on the surface of the sialidase molecule. These mutations dramatically reduce the enzyme activity and cause a rapid intralysosomal degradation of the expressed protein. We hypothesize that this region may be involved in the interface of sialidase binding with lysosomal cathepsin A and/or β-galactosidase in their high-molecular-weight complex required for the expression of sialidase activity in the lysosome.

INTRODUCTION

Sialidosis (also called mucolipidosis I and cherry-red spot myoclonus syndrome) is an autosomal recessive lysosomal storage disease caused by the genetic deficiency of lysosomal sialidase activity (reviewed in refs 1–3). It is characterized by tissue accumulation and urinary excretion of sialylated oligosaccharides and glycoproteins (1). Sialidosis is subdivided into two main clinical variants with different age of onset and severity. Sialidosis type I or non-dysmorphic type is a late-onset mild form, characterized by bilateral macular cherry-red spots, progressive impaired vision and myoclonus syndrome (4–8). Sialidosis type II or dysmorphic type is the infantile-onset form, which is also associated with skeletal dysplasia, Hurler-like phenotype, dysostosis multiplex, mental retardation and hepatosplenomegaly (9–12). A severe form of the disease manifests prenatally and is associated with ascites and hydrops fetalis (13–15). The age of onset and severity of the clinical manifestations correlate with the amount of residual sialidase activity, suggesting the existence of considerable genetic heterogeneity (1–3).

An understanding of the molecular defects and biochemical mechanism of sialidosis became possible after the recent cloning of the sialidase gene and characterization of the protein in our laboratory and others (16–19). Previously, we have identified a frameshift mutation caused by an ACTG duplication after nucleotide 7 (7insACTG) and two missense mutations, 779T→A (Phe260Tyr) and 1088T→C (Leu363Pro), in sialidosis type II patients (17). Bonten *et al*. (18) identified a 1258G→T transversion, which introduced a premature stop codon and the C-terminal truncation of 38 amino acids in two

+Present address: The Scripps Research Institute, La Jolla, CA 92037, USA
§To whom correspondence should be addressed. Tel: +1 514 345 4931/2736; Fax: +1 514 345 4801; Email: alex@justine.umontreal.ca

siblings with type I sialidosis. They also described a 401T→G transversion (Leu91Arg) and a 1337delG deletion that caused a frameshift and extended the protein by 69 amino acids in a type II patient. In addition to mutations identified in humans, a 625C→A (Leu209Ile) change in the sialidase gene was reported in the SM/J mouse strain, characterized by reduced sialidase activity in selected tissues (20,21). The biochemical consequences of some of the identified missense mutations (like Phe260Tyr or Leu209Ile) are difficult to explain since they do not affect the putative active site residues of the enzyme and are not expected to introduce significant change in the conformation of the enzyme.

We screened the genomic DNA of nine patients of diverse ethnic origin affected by type I and type II forms of sialidosis for the mutations in the sialidase gene. To prove that the identified changes cause the deficiency of sialidase, we expressed the variants in COS-7 cells. We have identified six new missense mutations and localized them in the modeled tertiary structure of sialidase. We found that most of the mutations causing a severe type II sialidosis are clustered in one region of the sialidase molecule, suggesting that this region may be involved in the sialidase binding interface with the lysosomal multienzyme complex, also containing β-galactosidase and cathepsin A.

RESULTS

Sequence of the sialidase gene

Although the structures of the human and mouse sialidase genes were reported previously (19,21,22), the sequences of the splice junctions did not extend far enough into the introns to provide the selection of the oligonucleotide primers suitable for amplification of sialidase exons. To determine the intronic sequence of the sialidase gene, we amplified the entire gene in four overlapping fragments using genomic human DNA and cDNA primers complementary to exon sequences (Fig. 1). Those were subcloned into pCR2.1 vector and sequenced. We found that intron 1 (424 bp) starts after nucleotide 159 in the cDNA, intron 2 (547 bp) after nucleotide 352, intron 3 (564 bp) after nucleotide 615, intron 4 (174 bp) after nucleotide 798 and intron 5 (96 bp) after nucleotide 1021 (Fig. 1). The total length of the gene from the initiating to the stop codon is 3.051 kb. The sequences of the intron–exon junctions were in agreement with those reported by Milner *et al.* (19). The positions and sequences of the oligonucleotide primers chosen to amplify each of six exons of the sialidase gene and the flanking intron sequences are shown in Figure 1.

Identification of mutations in the sialidase gene

DNA of nine sialidosis patients (Table 1), representing a total of 18 disease alleles, was analyzed. Seven patients were diagnosed with severe, infantile-onset type of sialidosis (type II) and two patients had the mild juvenile-onset type of disease (type I) (23–28). For the mutation analysis, the exons of the sialidase gene and flanking intron regions were amplified by polymerase chain reaction (PCR). The analysis of the PCR products using agarose gel electrophoresis (data not shown) demonstrated products of the expected size in all patients. The fragments were studied by single-strand conformation polymorphism (SSCP) analyses (29). [^{35}S]dATP- or [^{35}P]dATP-labeled PCR fragments were denatured and separated on polyacrylamide gel with and without 10% glycerol. Band patterns were compared between normal and mutant DNA. Differences were observed in fragments containing exon 2 of sialidosis patient 6, exon 3 of patient 4, exon 4 of patients 1, 2 and 5, and exon 5 of patients 3, 7, 8 and 9 (data not shown). These fragments were sequenced (Fig. 2). The results of the mutation analysis are summarized in Table 2.

Sequencing of exon 4 from an infant of Turkish origin born of consanguineous parents (patient 5) revealed that the patient is homozygous for a frameshift mutation: a deletion after nucleotide 623 (623delG). This mutation results in a premature stop codon at nucleotide 904, and early truncation of sialidase protein at residue 301. To confirm the inheritance of the mutation, we studied parental DNA. Direct sequencing of the corresponding regions of the PCR-amplified fragments (data not shown) resulted in the appearance of ambiguous sequence following the frameshift site, suggesting that both parents are heterozygous for the 623delG mutation. This finding justifies the complete absence of sialidase activity in the patient's cultured fibroblasts.

In two sibs of Spanish origin (patients 7 and 8), we have identified an 808C→T homozygous nucleotide change resulting in Leu270Phe amino acid substitution. The 808C→T mutation removed an *Sal*I restriction site, which was used to confirm the mutation (Fig. 3, top right). The *Sal*I site was absent in both alleles of patients 7 and 8, in one allele of their parents, but not in any of 20 normal chromosomes tested.

Sequencing of exon 4 in patients 1 and 2, of Caucasian origin from Mexico and the USA, revealed that both are homozygous for a 679G→A nucleotide change resulting in Gly227Arg mutation. This change removes an *Mae*II restriction site in the genomic DNA PCR product of patients 1 and 2, but not of any of 20 normal subjects (Fig. 3, top left).

Exon 2 of patient 6 contained a homozygous G203T mutation substituting Gly68 for Val. Exon 3 of patient 4 contained a homozygous 544A→G (Ser182Gly) change and exon 5 of patient 3 contained a homozygous 893C→T (Ala298Val) change. Since all of these mutations did not alter any known restriction site, they were confirmed by allele-specific oligonucleotide hybridization (ASO). All 40 alleles from 20 unrelated normal controls were all negative for these nucleotide changes (Fig. 3, bottom).

Exon 5 of patient 9 contained one copy of a 982G→A substitution, which changes Gly328 to Ser. This change was also confirmed by ASO. Both the normal and mutant oligonucleotide probes hybridized with the exon 5 amplification product of patient 9, whereas only the normal primer hybridized with the exon 5 amplification product of 20 normal subjects (data not shown). A mutation in the second allele of this patient has not been identified so far.

Two different sialidosis-related diseases are presently listed in the Mendelian Inheritance in Man (MIM) database, whose relationships have, until now, been unclear. These are neuraminidase deficiency (MIM 256550) and nephrosialidosis (MIM 256150). In addition, Goldberg syndrome or galactosialidosis (MIM 256540) presents as a combined deficiency of sialidase and β-galactosidase activities. Patient 6 studied in this paper (27) appears to be a well documented case of nephrosialidosis, whereas all others were diagnosed as having type I, type II or

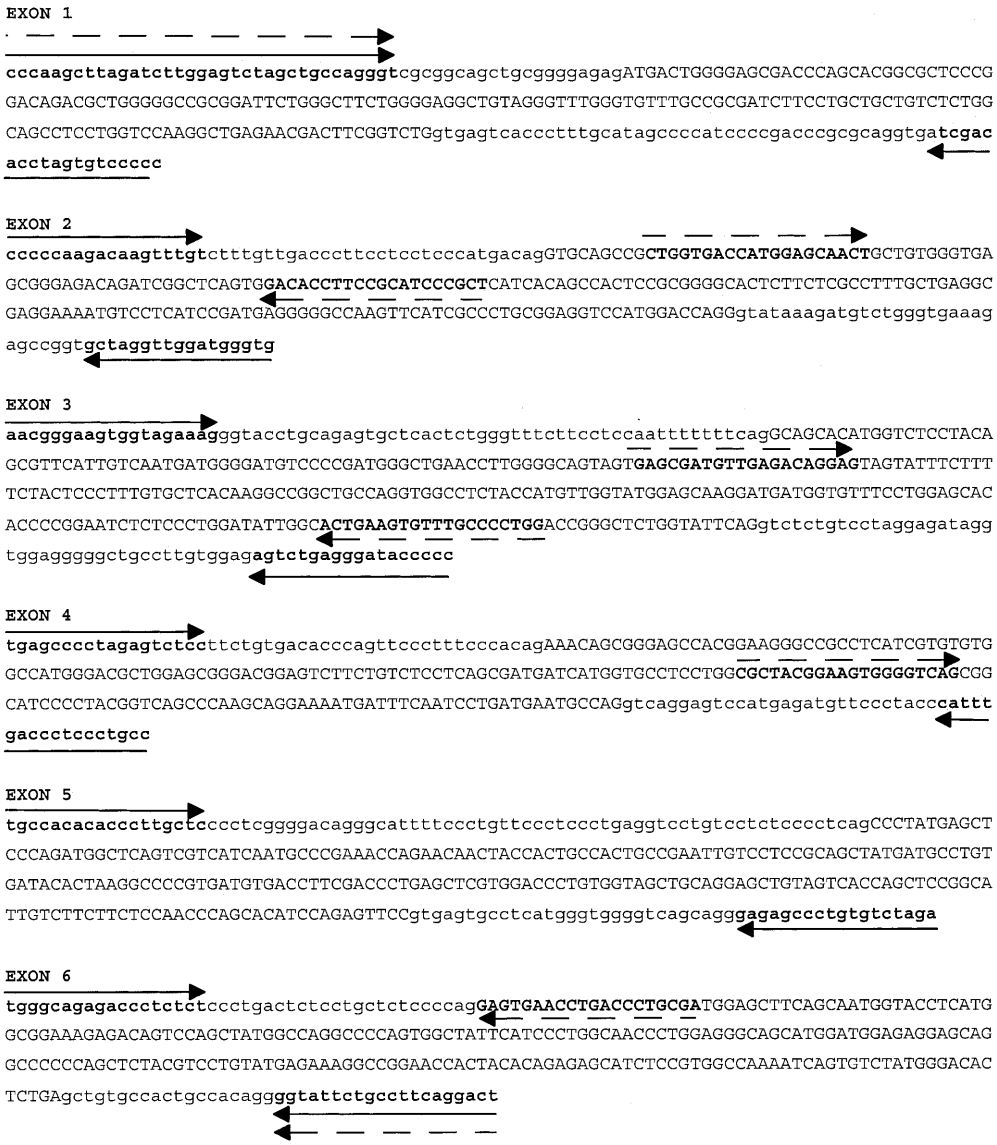

Figure 1. Nucleotide sequence of the intron/exon splice sites of human sialidase gene and their flanking regions. Exonic sequence is shown in uppercase letters and intronic sequence in lowercase letters. Positions of the oligonucleotide primers used to amplify the exons and genomic fragments of sialidase are shown by solid and dashed arrows, respectively, and their sequences are given in bold.

congenital sialidosis. The original patient of Goldberg, who was previously reported to have neuraminidase deficiency rather than galactosialidosis (23), is patient 1 in this report. Therefore, our data indicate that the various forms of isolated sialidase deficiencies, from the most severe to the mildest, are in fact allelic and are caused by the mutations in the lysosomal sialidase gene.

Expression analysis

The functional significance of new mutations was assayed by transient expression of the mutant cDNA. In addition to six point mutations identified in this study, we also expressed sialidase 779T→A (Phe260Tyr) and 1088T→C (Leu363Pro) mutants that we have described previously (17). Mutations were generated by site-directed mutagenesis in the pCMV-SIAL vector previously used for the expression of sialidase (17). Short restriction cassettes containing the mutations were then inserted into the parental pCMV-SIAL vector replacing the corresponding fragments of wild-type sialidase cDNA. The inserts and junction regions of the resulting constructs were verified by sequencing to ensure the correct introduction of mutations. Mutant or wild-type sialidase was co-expressed with human cathepsin A (CathA), which is necessary for the expression of sialidase activity. We used for transfection both COS-7 cells and papilloma virus-immortalized cultured skin fibroblasts of a sialidosis type II patient (line WG0544), characterized by very low sialidase mRNA level and activity (17). Forty-eight hours after transfection, the cell lysates were assayed for sialidase, CathA and control β-hexosaminidase activities.

The expression results are shown in Figure 4. All transfected cells had similar CathA activity, suggesting the same transfection efficiency for all cells. Five of the expressed mutants,

Table 1. Sialidosis patients

Patient	Ethnicity	Gender	Age at diagnosis (years)	Diagnosis	Sialidase activity in fibroblasts (% of normal)	Comment	Reference
1	Mexican	Male	20	Sialidosis type II	2–17	β-galactosidase, 200%; consanguineous ancestry; cherry-red spots; seizures, myoclonus; mental retardation	23
2	American (Caucasian)	Male	14	Sialidosis type II	12	Hurler-like face; skeletal abnormalities; mental retardation; cherry-red spots	24
3	Ashkenazi Jewish	Female	3 months	Sialidosis type II	0–3	β-galactosidase, normal; 4 sibs, all affected; seizures; hydrops fetalis; hepatosplenomegaly	25
4	Chinese	Male	24	Sialidosis type I	2–6	Myoclonus; mild dysphagia; normal leukocyte sialidase and oligosaccharide pattern	26
5	Turkish	Female	1	Sialidosis type II	0	β-galactosidase normal; consanguineous ancestry; hydrops fetalis; skin desquamation; healthy sister; died at 82 days	NA
6	Polish	Male	4.5	Sialidosis type II	7–8	β-galactosidase normal; consanguineous ancestry; hydrops fetalis; nephrosialidosis, first in Poland; cherry-red spots	27
7	Spanish	Male	10	Sialidosis type II	1–2	Brother of patient 8; consanguineous ancestry	NA
8	Spanish	Female	18 months	Sialidosis type II	0	Sister of patient 7; consanguineous ancestry; hydrops fetalis; died at 2 years	NA
9	Italian	Female	23	Sialidosis type I	2–6	β-galactosidase, normal; healthy until 17 years, ataxia; seizures, myoclonus; cherry-red spots; slight mental deterioration	(28)

NA, not applicable.

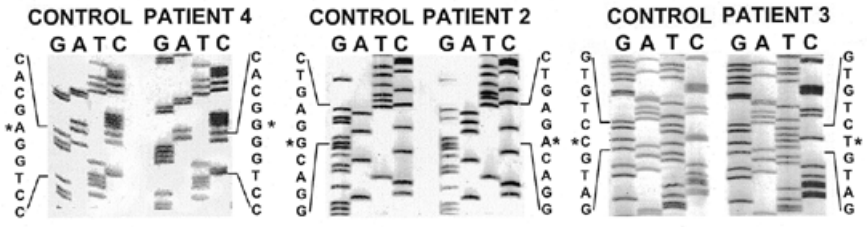

Figure 2. Examples of the mutation detection in the sialidase gene. Direct sequence of mutant and normal DNA, showing the presence of mutation 544A→G in exon 3 of the sialidosis patient 4 (left), 679G→A in exon 4 of patient 2 (middle) and 893C→T in exon 5 of patient 3 (right). Positions of mutations are indicated with asterisks.

Gly68Val, Gly227Arg, Ala298Val, Gly328Ser and Leu363Pro, had very low (<10% of normal) or absent sialidase activity (Fig. 4A). The activity of Phe260Tyr and Leu270Phe mutants was between 10 and 20% of normal, and that of the Ser182Gly mutant was between 20 and 40% of normal (Fig. 4A). Additional experiments showed that Leu270Phe and Phe260Tyr mutants were also significantly less stable than the wild-type sialidase. The half-life of their enzymatic activity in cellular lysates at 37°C was ~30 min as compared with the 2 h half-life of the wild-type enzyme.

The expressed sialidase protein was studied by western blotting (Fig. 4B). In the cells co-transfected with wild-type sialidase and CathA cDNA, we observed a double band of 48.3 and 46 kDa proteins, a product previously identified as a mature active sialidase (30). The same pattern was observed in the cells transfected with Ser182Gly mutant, suggesting that the protein reaches the lysosomes, and is correctly processed and stable. In contrast, in the cells transfected with the Gly227Arg and Leu363Pro mutants, the anti-sialidase antibodies reacted with two high molecular weight (62 and 70 kDa) bands, suggesting that most of the protein is retained in pre-lysosomal compartments. In the cells transfected with Gly328Ser, Ala298Val, Leu270Phe, Gly68Val or Phe260Tyr mutants, the antibodies detected both mature processed sialidase protein

Table 2. Mutations identified in the sialidase gene

Patient	Site	Nucleotide change[a]	Method of confirmation	Putative consequence
1 and 2	Exon 4, codon 227	679G→A	REA	Gly227Arg
3	Exon 5, codon 298	893C→T	ASO	Ala298Val
4	Exon 3, codon 182	544A→G	ASO	Ser182Gly
5	Exon 4, codon 208	623delG		Frameshift, Stop904
6	Exon 2, codon 68	203G→T	ASO	Gly68Val
7 and 8	Exon 5, codon 270	808C→T	REA	Leu270Phe
9	Exon 5 Codon 328	982G→A	ASO	Gly328Ser

[a]Patients 1–8 are homozygous with the mutations identified in heterozygous form in both parents. Patient 9 is a compound heterozygote.

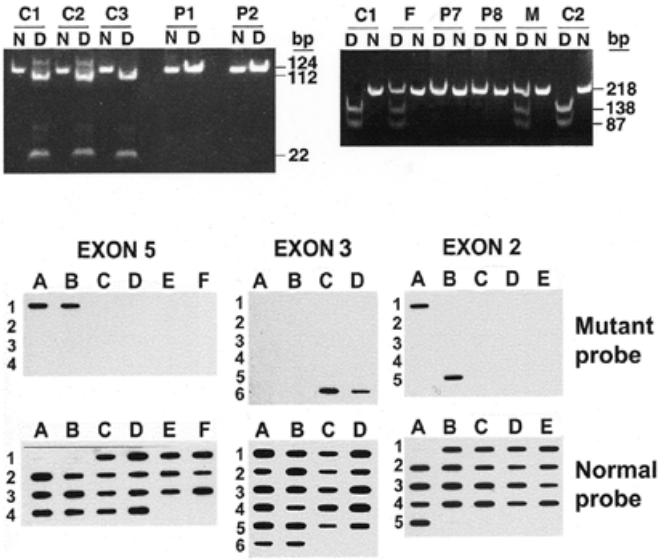

Figure 3. Examples of the mutation confirmation by REA or ASO. (Top left) 679G→A mutation destroyed an *Mae*II site in the genomic DNA PCR product of patients 1 and 2 (P1 and P2), but not of normal subjects (C1, C2 and C3). D, DNA sample digested; N, not digested with a restriction enzyme. (Top right) 808C→T mutation destroyed an *Sal*I site in one allele of the genomic DNA PCR product of both the mother and father of patients 7 and 8 (M and F), in both alleles of patients 7 and 8 (P7 and P8), but not in normal controls (C1 and C2). (Bottom) Only the oligonucleotide probes containing 893C→T, 544A→G and 203G→T mutations, respectively, hybridized with the exon 5 amplification product of patient 3 (left, positions A1, B1), exon 3 amplification product of patient 4 (middle, positions C6, D6) and exon 2 amplification product of patient 6 (right, positions A1, B5). Only the normal primers hybridized with the corresponding amplification products of 20 normal subjects (left, positions C1–D4; middle, positions A1–B6; right, positions B1–E5).

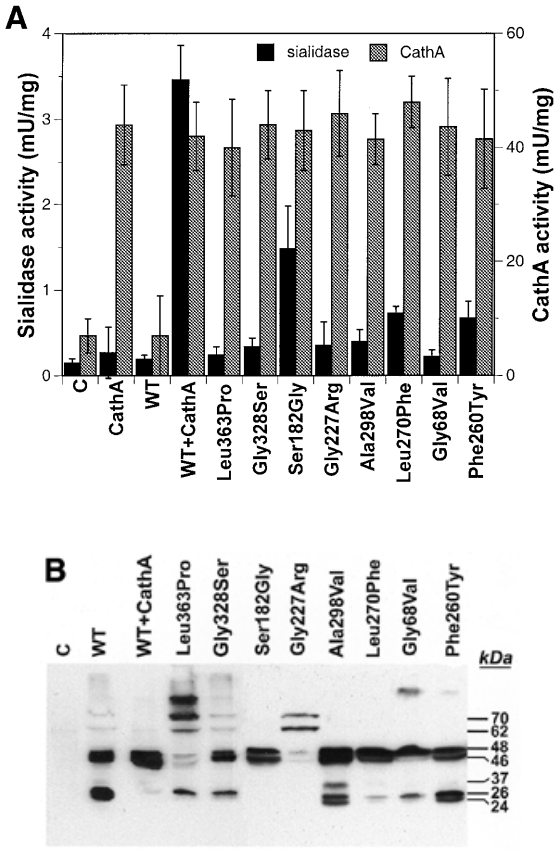

Figure 4. Expression of mutant sialidase in COS-7 cells. (**A**) Sialidase and CathA activities in cellular lysates of COS-7 cells measured 48 h after co-transfection with CathA and mutant sialidase cDNA. Cells were transfected and enzyme activities assayed as described in Materials and Methods. Values represent means ± SD of triplicate experiments. CathA, cells transfected with the CathA cDNA only; WT, cells transfected with the wild-type sialidase cDNA; WT + CathA, cells co-transfected with the wild-type sialidase and CathA cDNA; C, control COS-7 cells. Enzyme activities in the cell lysates were determined 48 h after transfection. Values represent means ± SD of five independent experiments. The expression studies performed with cultured skin fibroblasts of the sialidosis patient WG0544 produced similar results (data not shown). (**B**) Detection of sialidase in the cellular lysates of COS-7 cells co-transfected with CathA and mutant sialidase cDNA by western blotting. Lysate aliquots (20 µg of protein) were subjected to SDS–PAGE, transferred to a nitrocellulose membrane and stained with rabbit anti-sialidase antibodies as described. Samples are indicated as in (A).

and several proteins with lower molecular masses (37, 26 and 24 kDa). These proteins, also found in the cells transfected with wild-type sialidase in the absence of CathA (Fig. 4B), probably represent fragments of sialidase molecule, suggesting the rapid proteolytic degradation of mutant sialidase in the lysosome. Immunolabeling of the sialidase mutants expressed in COS-7 cells (data not shown) confirmed its intracellular localization suggested on the basis of the western blots. Leu363Pro and Gly227Arg mutants showed mostly a diffuse cytoplasmic localization, whereas in the case of all other mutants anti-sialidase immunofluorescence was observed in

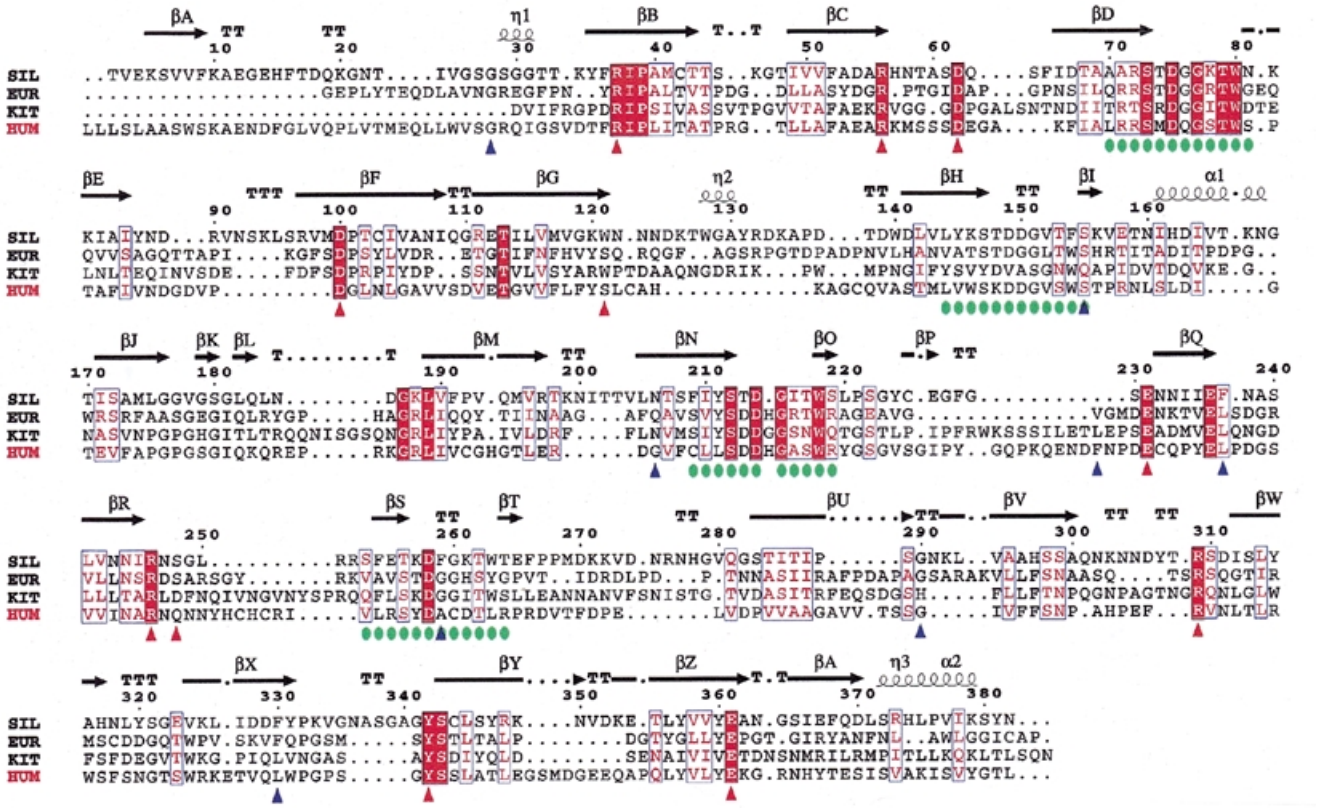

Figure 5. Amino acid sequence alignment of human lysosomal sialidase (HUM; residues 36–415) with homologous sialidases from *V.cholerae* (KIT), *M.viridifaciens* (EUR) and *S.typhimurium* (SIL). The identical residues are shown as white on red. Homologous residues are shown in red and boxed. Indicated above the alignment are the secondary structural elements of the structure of bacterial sialidases (33–35); α-helixes are indicated by 'spirals', β-sheets by arrows and turns by 'T'. Beneath the alignment, the positions of active site residues (red triangles), mutations identified in human sialidase gene (blue triangles) and 'Asp-box' repeats (green dots) are indicated.

perinuclear punctate structures co-localized with lysosomal marker LAMP2.

Structural model of sialidase

The structural model of lysosomal sialidase was built using the atomic coordinates of homologous sialidases from *Micromonospora viridifaciens* (EUR), *Salmonella typhimurium* (SIL) and *Vibrio cholerae* (KIT) as templates. These structures were superimposed to determine structurally conserved regions (SCRs). The sequence of human neuraminidase was then aligned with the SCRs (Fig. 5).

Analysis of the deduced structure (Fig. 6) indicates that human lysosomal sialidase shares the same fold as bacterial and viral sialidases. This fold consists of six four-stranded antiparallel β-sheets arranged as the blades of a propeller around a pseudo six-fold axis (31–33). Viral sialidases are tetramers of four identical β-propellers (31), whereas some bacterial sialidases contain additional domains built around the central canonical fold (34,35). These additional domains are usually involved in carbohydrate recognition (34,35). The model reveals that human lysosomal sialidase does not contain similar domains. This suggests that other components of the multienzyme lysosomal complex may be responsible for previously observed binding of the sialidase to lysosomal and plasmatic membranes (30).

Despite the low sequence identity (15% between the bacterial and viral sialidases, and ~30% between different bacterial sialidases), the topology of the catalytic domain and the active site residues are strictly conserved in these enzymes. The model indicates that this architecture of the active site is also conserved in human sialidase (Table 3). In particular, the Arg78 in human enzyme that is found in an RIP/RLP motive motif (REP in viral enzymes) is probably one of the residues responsible for binding the sialic acid carboxylate group. The other two Arg residues that stabilize the carboxylic group in the active site are potentially Arg280 and Arg341 (Table 3). Finally, the conserved Asp135 in the human enzyme is in the proper location to bind the *N*-acetyl-/*N*-glycolyl group of the substrate [Asp292, Asp131 and Asp100 in *V.cholerae*, *M.viridifaciens* and *S.typhimurium*, respectively (Table 3)]. This Asp residue is not conserved in the influenza enzyme, the substituted residue creates a pocket that can bind the guanidinium group of a 4-guanidino-Neu5Ac2en (36), a highly specific inhibitor of viral enzyme widely studied as a potential anti-influenza drug (reviewed in ref. 37). Our model indicates that this class of influenza sialidase inhibitors should not, therefore, affect the endogenous human lysosomal enzyme. The Glu394 residue that stabilizes the position of Arg78 through a hydrogen bond, as well as Tyr370 and Glu264 that are connected by a hydrogen bond and may donate a proton in

Table 3. Conserved active site residues between sialidases from *V.cholerae* (KIT), *M.viridifaciens* (EUR), *S.typhimurium* (SIL) and human lysosomal sialidase (HUM)

KIT	EUR	SIL	HUM
R224	R68	R37	R78
R245	R87	R56	R97
D250	D93	D62	D103
D292	D131	D100	D135
W311	S150	W121	S156
N318	–	T127	–
E619	E260	E231	E264
R635	R276	R246	R280
D637	S278	S248	Q282
R712	R342	R309	R341
Y740	Y370	Y342	Y370
E756	E386	E361	E394

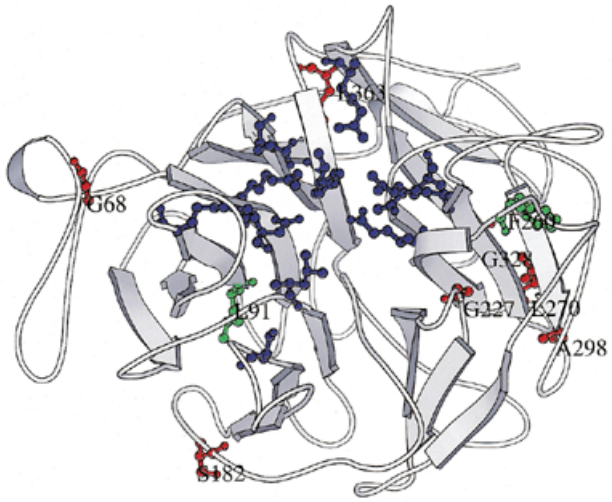

Figure 6. Ribbon drawing of the human lysosomal sialidase model showing the location of six new (red) and three previously identified (green) (17,18) point mutations. The deduced active site residue side chains are shown in blue.

the process of substrate hydrolysis (33–35), are also conserved. Asp103 is either a donor of the proton for the glycosidic bond or a stabilizer of the proton-donating water molecule.

The repeated so-called 'Asp-box' motifs (Ser/Thr-X-Asp-X-Gly-X-X-Trp/Phe) are also structurally conserved in human sialidase (Fig. 5). These repeats, found in all bacterial and mammalian sialidases, are always located between the third and the fourth β-strand at each sheet (βD and βE, βH and βI, βN and βO, and finally βS and βT). All Asp-boxes always have a similar arrangement with the aromatic residues packed into the hydrophobic core stabilizing the turn, whereas the hydrophilic Asp residues are solvent exposed. Gaskell *et al.* (34) have reported that similar motifs are also present at topologically conserved positions in eight-bladed β-propeller structure of bacterial methanol and methylamine dehydrogenases as well as seven-bladed fungal galactose and glyoxal oxidases, suggesting that these enzymes have evolved from the same four-bladed precursors through a gene duplication.

Potential effects of mutations and their correlation with enzymatic activity and patient phenotype

The Gly227Arg substitution was identified in two unrelated sialidosis type II male patients 1 and 2 of Caucasian origin from Mexico and the USA. Both patients were homozygous for this mutation and had a low residual level of sialidase activity in the cells. Our expression studies showed that the Gly227Arg mutant does not have enzymatic activity and lacks normal processing or lysosomal targeting. Gly227 is located in a βN strand of the sialidase molecule (second strand of the third sheet) and is not conserved in bacterial sialidases. Although such a substitution of a small neutral residue for a large charged one has the potential of greatly affecting the structure of the enzyme, we could not directly explain the clinical severity of the mutation with the model.

The Ala298Val (893C→T) mutation was found in both alleles of a sialidosis type II patient of Ashkenazi Jewish origin, whose severe phenotype and low residual cellular sialidase activity correlated with the expression results that showed a complete loss of the enzyme activity (Fig. 4). Our structural model indicates that Ala298 is situated in an 'Asp-box' repeat in the center of a turn loop between the third and the fourth strands of the fourth β-sheet (Fig. 6). The location of this mutation, in a surface loop, is consistent with expression studies which showed normal targeting and processing of the enzyme incompatible with a fold defect (Fig. 4).

Gly68Val substitution was found in both alleles of a patient of Polish origin who presented the severe clinical variant of sialidosis. In accordance with the clinical data, the Gly68Val sialidase mutant did not express any activity in COS-7 cells or in human fibroblasts (Fig. 4A). Gly68, which is conserved in the sialidases from *Micromonospora* and *Salmonella*, is a part of the short α-helix located between the first and the second β-strand. The low sequence homology in this region of the model did not permit us to draw conclusions on the possible structural effect of this mutation.

A Leu270Phe change was identified in two sibs of Spanish origin diagnosed with type II sialidosis. Both patients are homozygous for the mutation and have very low sialidase activity in their cells. Our expression studies showed that the Leu270Phe mutant is properly targeted and processed, has ~20% of the normal activity, but is significantly less stable than the wild-type enzyme (Fig. 4). Such low stability could result in almost complete sialidase deficiency in the cells of the affected patients and explains their severe clinical phenotype. In the human sialidase model, Leu270 is found at the end of the βQ strand. Although this Leu is conserved in both the *Micromonospora* and *Vibrio* enzymes, it was interesting to find a Phe residue in this position in *Salmonella*. Moreover, the CA of the Phe residue in *Salmonella* is shifted by 1.5 Å compared with the other two bacterial structures. Together, these results indicate that a Phe at this position can be accommodated, but with a significant structural shift which is consistent with the expression results and may explain the low stability of this mutant.

Previously, we have described a sialidosis type II patient (17), heterozygous for Phe260Tyr and Leu363Pro mutations.

The Phe260Tyr and Leu270Phe residue mutations are located at the opposite ends of the same βQ strand as a Leu270Phe mutation, but cause similar effects on the enzyme. The mutant products are normally targeted and processed, but are unstable and rapidly degrade in the lysosome. Phe260 is located in a surface 'loop' region in the model that does not exist in the other structures. Therefore, the only conclusion that may be deduced from the model is that this residue is probably accessible for binding other protein.

In contrast, the Leu363Pro mutant is retained in pre-lysosomal compartments and most probably lacks the proper fold. Leu363 is located in the center of the βX strand. A hydrophobic Leu (*Vibrio*) or Phe (*Micromonospora* and *Salmonella*) residue is found in this position in the bacterial structures. Substitution of this Leu for a Pro residue in either the model structure or in the *Vibrio* structures results in a steric clash with the backbone carboxylate of residue Leu344 or Leu715 located in the adjacent βW strand.

The Gly328Ser mutation found in one allele of a sialidosis type I patient of Italian origin is located in a highly variable turn loop region that bridges between the βU strand and the βV strand (the first and the second strands of the fifth β-sheet). Gly at this position is conserved in human, *Salmonella* and *Micromonospora* enzymes. The expressed product was targeted to the lysosomes and correctly processed, but showed <2% of the residual activity. It is tempting to speculate that the mutation in the second allele of the patient, which we were unable to identify, determines the mild phenotype with a late onset and a moderate clinical course.

The sialidosis type I patient of Chinese origin was homozygous for a Ser182Gly point mutation. Ser182 conserved in both sialidases from *M.viridifaciens* and *S.typhimurium* (Fig. 5) is located at the end of the second 'Asp-box' repeat. In our model, Ser182 is completely solvent accessible and located at the base in a long flexible surface loop. This may explain the relatively high (~40% of normal) activity expressed by the Ser182Gly sialidase mutant and correlates with the mild clinical phenotype of the patient.

DISCUSSION

Lysosomal sialidase has a unique feature, which distinguishes it from homologous non-lysosomal sialidases as well as from other lysosomal enzymes. Its functional activity absolutely depends on the integrity of the sialidase association with a multienzyme lysosomal complex containing cathepsin A/protective protein (CathA), β-galactosidase (GAL) and *N*-acetylgalactosamine-6-sulfate sulfatase (GALNS) (38–40). The complex protects sialidase and GAL against rapid proteolysis (30,38,41), and supports their catalytically active conformations (39,42). It was also reported that the association of CathA with Gal and sialidase provides proper targeting and processing of their precursors (43–45). In the autosomal recessive disease, galactosialidosis, a primary genetic defect of CathA (38,41) results in disruption of the complex and causes the combined deficiency of both GAL and sialidase activities. The clinical features and a composition of storage products in galactosialidosis resemble those in sialidosis (8,9,46). One may hypothesize that mutations in sialidase that destabilize its association with the complex can be 'lethal' for the enzyme even though they do not directly affect activity or stability of sialidase.

Results obtained in this study support this hypothesis. Six of nine sialidosis patients studied here had point mutations in the sialidase cDNA, leading to amino acid substitutions (Table 2). To understand the influence of these mutations on sialidase function, we have modeled the tertiary structure of human sialidase and located the identified mutations. None of the mutations directly affected the deduced active site residues or were found in the central core of the sialidase molecule, but all of them involved residues on the surface of the enzyme. Therefore, in most cases it is unlikely that these mutations would introduce electrostatic or steric clashes in the protein core leading to general folding defects of the sialidase and its retention in the ER/Golgi compartment as was observed for most of the mutations affecting CathA (47). Indeed, the expressed mutant products of sialidase were targeted to lysosomes, with the exception of the Gly227Arg and Leu363Pro mutants for which both western blotting and immunolabeling suggested misfolding and retention in the pre-lysosomal compartments. Moreover, structural analysis showed that five of the eight missense mutations, Gly227Arg, Ala298Val, Leu270Phe, Phe260Tyr and Gly328Ser, are clustered in one region on the surface of the sialidase molecule (Fig. 6). Western blot analysis demonstrated that Ala298Val, Leu270Phe, Phe260Tyr and Gly328Ser mutants expressed in COS-7 cells undergo normal intralysosomal processing, but then are rapidly degraded to smaller 37, 26 and 24 kDa fragments similar to those observed in COS-7 cells in which the wild-type sialidase was expressed in the absence of human CathA. We have previously observed exactly the same pattern of degradation products when we have expressed the wild-type human sialidase in the cells of a galactosialidosis patient, which lack CathA (30). Metabolic labeling studies (30) also demonstrated the dramatically reduced half-life of the 48.3 kDa active form of sialidase in galactosialidosis cells (30 min versus 2.7 h in normal cells), similar to that observed in this work (30). Together, these results permit us to speculate that the identified surface region where most mutations were found may represent part of the interface of sialidase binding with CathA and/or GAL in the lysosomal multienzyme complex (38,39). The data obtained will help to clarify the basic mechanism of the enzyme function in the lysosome and open the possibility to address directly the question of the supramolecular organization of the multienzyme lysosomal complex.

MATERIALS AND METHODS

Patients

All patients were clinically and biochemically diagnosed as having sialidosis. Available clinical data are presented in Table 1. Genomic DNA was purified either from the blood of patients or from their cultured skin fibroblasts as described previously (48).

Cloning of the sialidase gene and sequencing of sialidase introns

The sialidase gene was amplified in four overlapping fragments using genomic DNA from human placenta and oligo-

nucleotide primers complementary to exon sequences (Fig. 1). The amplified DNA fragments were purified using the Qiaquick PCR purification kit (Qiagen, Mississauga, Ontario) and cloned into pCR2.1 vector using the TA cloning kit (InVitrogen, San Diego, CA) according to the manufacturer's protocol. Plasmid DNA was extracted using alkaline lysis (48) and automatically sequenced using the PRISM Ready Reaction Dye Deoxy Terminator cycle sequencing kit on an Applied Biosystems 373A automated sequencer.

Amplification of sialidase exons

The oligonucleotide primers for the amplification of sialidase exons and adjacent splicing regions were selected at least 40 bp upstream of the acceptor splice sites and at least 40 bp downstream of donor sites. For some exons, more than one primer combination was tested to find one that produced a specific amplification of the exon. Sequences and positions of the primers used to amplify the exons are shown in Figure 1. The amplification conditions were: denaturation at 95°C for 2 min, 32 cycles, each consisting of 30 s at 95°C; 30 s at 54°C for exons 2 and 3, 56°C for exon 5 and 58°C for exons 1, 4 and 6, respectively; 1 min at 72°C followed by 10 min at 72°C.

Screening for previously undescribed mutations

Because of the small size of the exons, they were directly analyzed by SSCP as described (29,49). Typically, a 5–10 µl aliquot of the labeled PCR product was mixed with an equal volume of 95% formamide, 20 mM EDTA, 0.05% bromophenol blue, 0.05% xylene-cyanol FF. The sample was denatured by heating at 95°C for 3 min, rapidly cooled in an ice bath for 2 min and immediately loaded onto 0.4 mm × 31 cm × 38 cm 6% polyacrylamide gels containing 10 or 0% glycerol. Gels were run overnight at 10°C and 6 W constant power, or for ~3 h at 25°C and 30 W constant power, vacuum dried at 80°C and analyzed by autoradiography. Non-denatured samples were run beside denatured samples.

Exons and adjacent splicing regions for which the SSCP analysis produced band shifts or gain or loss of bands compared with normal controls, suggesting the presence of mutations, were manually sequenced using the Thermo Sequenase radiolabeled terminator cycle sequencing kit (Amersham Life Science, Cleveland, OH).

Confirmation of mutations

For previously undescribed mutations, the nucleotide changes were confirmed directly in PCR-amplified products from genomic DNA. If the mutation created or destroyed a restriction enzyme site, restriction enzyme digestion was used to confirm the presence of the mutation. A 10–12 ng aliquot of the normal and mutant amplification product was digested with the appropriate restriction enzyme (*Sac*I for exon 5 of patients 7 and 8 or *Mae*II for exon 4 of patients 1 and 2) in a 15 µl volume for 1–2 h and analyzed by electrophoresis in 8% polyacrylamide gel containing ethidium bromide as described previously (48).

Mutations that did not create any changes in restriction enzyme sites were confirmed by ASO hybridization (48). The fragments surrounding mutations were amplified from genomic DNA of the patients and of 20 unrelated normal individuals, blotted on Zeta-Probe membrane (Bio-Rad, Hercules, CA) and hybridized with oligonucleotides complementary to normal and mutant DNA sequence, respectively (Table 4). The hybridization mixture typically contained 5 pmol of ^{32}P-labeled mutant probe and 50 pmol of normal unlabeled oligonucleotide or vice versa.

Table 4. Mutagenic and selection oligonucleotides used for site-directed mutagenesis

Mutation	Mutagenic oligonucleotide
G679A	5′-CTG GAG CGG GAC AGA GTC TTC TCT-3′
C893T	5′-AGC TAT GAT GTC TGT GAT ACA-3′
A544G	5′-GTT TCC TGG GGC ACA CCC CGG-3′
G203T	5′-GTG GGT GAG CGT GAG ACA GAT CGG-3′
C808T	5′-GCC CTA TGA GTT CCC AGA TGG-3′
G982A	5′-CAC CAG CTC CAG CAT TGT CTT C-3′
T779A	5′-AGG AAA ATG ATT ACA ATC CTG ATG-3′
T1088C	5′-AGA CAG TCC AGC CAT GGC CAG GCC-3′
Selection oligonucleotide	5′-GTG ACT GGT GAG GCC TCA ACC AAG TC-3′

The underlined nucleotides represent the bases changed during mutagenesis.

Construction of mutant sialidase expression vector

Site-directed mutagenesis was performed using a Transformer Site-Directed mutagenesis kit (Clontech, Palo Alto, CA), previously described pCMV-SIAL expression vector, mutagenic primers corresponding to mutant sialidase sequences and a selection primer used to eliminate a unique *Sca*I restriction site in the vector (Table 4), according to the supplier's protocols. Briefly, all primers were phosphorylated enzymatically and, for each mutant, the corresponding mutagenic primer and the selection primer were annealed to heat-denatured pCMV-SIAL plasmid. After elongation by T4 DNA polymerase, ligation and primary digestion with *Sca*I restriction enzyme to linearize all non-mutated DNA, the plasmid pool was used to transform the *mutS* strain of BMH71-18. Plasmid DNA obtained from the pool of ampicillin-resistant transformants was subjected to a second *Sca*I digestion and transformed into *Escherichia coli* DH5α. Positive clones were selected after a final *Sca*I restriction analysis and the entire sialidase cDNA sequenced. Up to 80% of transformants contained the desired mutation. DNA fragments of between 300 and 600 bp containing the introduced mutations were obtained from the mutant pCMV-SIAL plasmids by double digestion with either *Bst*EII–*Nae*I, *Nae*I–*Kpn*I or *Kpn*I–*Eco*RV and subcloned into the parental pCMV-SIAL plasmid. The final constructs were verified by sequencing.

Expression of sialidase in COS-7 cells and sialidosis fibroblasts

COS-7 cells or cultured skin fibroblasts of the sialidosis patient WG0544 (17) were transfected with pCMV-SIAL and pCMV-CathA expression vectors using Lipofectamine Plus reagent (Life Technologies, Gaithersburg, MD) in accordance with the manufacturer's protocol. Forty-eight hours after transfection,

sialidase and control *N*-acetyl-β-glucosaminidase activities were assayed in cellular homogenates using the corresponding fluorogenic 4-methylumbelliferyl-glycoside substrates as described (50–52). The CathA activity was determined with CBZ-Phe-Leu (53). One unit of enzyme activity (U) is defined as the conversion of 1 μmol of substrate per minute. Proteins were assayed according to Bradford (54) with bovine serum albumin (Sigma, St Louis, MO) as standard. To measure the stability of the expressed sialidase, the cellular homogenate was incubated at 37°C for 30 min, 1, 2 and 3 h before the assay of sialidase activity.

Western blotting

SDS–PAGE of proteins in cellular homogenates was performed under reducing conditions according to the method of Laemmli (55). After electrophoresis, the proteins were electrotransferred to NITRO ME nitrocellulose membrane (Micron Separations, Westboro, MA). The sialidase detection on western blots was performed with anti-sialidase rabbit antibodies as described previously (30) using the BM Chemiluminescence kit (Boehringer Mannheim, Mannheim, Germany) in accordance with the manufacturer's protocol.

Immunofluorescent microscopy

COS-7 cells overexpressing wild-type and mutant sialidase were double stained with rabbit polyclonal anti-sialidase antibodies and monoclonal antibodies against lysosomal membrane marker LAMP2 (Washington Biotechnology, Baltimore, MD) and studied on a Zeiss LSM410 inverted confocal microscope (Carl Zeiss, Thornwood, NY) as described previously (22).

Modeling of sialidase tertiary structure

Modeling was performed using the structures of homologous sialidases from *M.viridifaciens* (32, PDB file 1eur.pdb), *S.typhimurium* (31, PDB file 2sil.pdb) and *V.cholerae* (33, PDB file 1kit.pdb) as templates. These structures were superimposed with ProSup King's Beech Biosoftware Solutions to determine SCRs. The sequence of human sialidase was manually aligned with the sequences of SCRs. The modeling was then carried out with Modeler 4 software (Andrej Sali, The Rockefeller University, New York, NY).

ACKNOWLEDGEMENTS

The authors thank Dr Roy Gravel for the help with DNA analysis and stimulating discussions, and Dr Mila Ashmarina for critical reading of the manuscript. This work was supported by the operating grants from the Medical Research Council of Canada, Fonds de La Recherche en Santé du Québec and Vaincre les Maladies Lysosomales Foundation (France) to A.V.P., and from NICHD Mental Retardation Research Center to G.T.

NOTE ADDED IN PROOF

The 808C→T (Leu270Phe) mutation was also found in two other unrelated sialidosis type II patients from the same region of Spain.

REFERENCES

1. Thomas, G.H. and Beaudet, A.L. (1995) Disorders of glycoprotein degradation and structure: α-mannosidosis, β-mannosidosis, fucosidosis, sialidosis, aspartylglucosaminuria and carbohydrate-deficient glycoprotein syndrome. In Scriver, C.R., Beaudet, A.L., Sly, W.S. and Vallee, D. (eds), *The Metabolic and Molecular Bases of Inherited Disease*. McGraw-Hill, New York, NY, pp. 2529–2561.
2. Federico, A., Battistini, S., Ciacci, G., de Stefano, N., Gatti, R., Durand, P. and Guazzi, G.C. (1991) Cherry-red spot myoclonus syndrome (type I sialidosis). *Dev. Neurosci*., **13**, 320–326.
3. Cantz, M. and Ulrich-Bott, B. (1990) Disorders of glycoprotein degradation. *J. Inherit. Metab. Dis.*, **13**, 523–537.
4. Durand, P., Gatti, R., Cavalieri, S., Borrone, C., Tondeur, M., Michalski, J.C. and Strecker, C. (1977) Sialidosis (mucolipidosis I). *Helv. Paediatr. Acta*, **32**, 391–400.
5. Sogg, R.L., Steinman, L., Rathjen, B., Tharp, B.R., O'Brien, J.S. and Kenyon, K.R. (1979) Cherry-red spot-myoclonus syndrome. *Ophthalmology*, **86**, 1861–1874.
6. Rapin, I., Goldfischer, S., Katzman, R., Engel Jr, J., and O'Brien, J.S. (1978) The cherry-red spot-myoclonus syndrome. *Ann. Neurol.*, **3**, 234–242.
7. O'Brien, J.S. (1979) The cherry red spot-myoclonus syndrome: a newly recognized inherited lysosomal storage disease due to acid neuraminidase deficiency. *Clin. Genet.*, **14**, 55–60.
8. Federico, A., Cecio, A., Battini, G.A., Michalski, J.C., Strecker, G. and Guazzi, G.C. (1980) Macular cherry-red spot and myoclonus syndrome. Juvenile form of sialidosis *J. Neurol. Sci.*, **48**, 157–169.
9. Till, J.S, Roach, E.S. and Burton, B.K. (1987) Sialidosis (neuraminidase deficiency) types I and II: neuro-ophthalmic manifestations. *J. Clin. Neuro-Ophthalmol*., **7**, 40–44.
10. Kelly, T.E. and Graetz, G. (1977) Isolated acid neuraminidase deficiency: a distinct lysosomal storage disease. *Am. J. Med. Genet.*, **1**, 31–46.
11. Oohira, T., Nagata, N., Akaboshi, I., Matsuda, I. and Naito, S. (1985) The infantile form of sialidosis type II associated with congenital adrenal hyperplasia: possible linkage between HLA and the neuraminidase deficiency gene. *Hum. Genet.*, **70**, 341–343.
12. Winter, R.M., Swallow, D.M., Baraitser, M. and Purkiss, P. (1980) Sialidosis type 2 (acid neuraminidase deficiency): clinical and biochemical features of a further case. *Clin. Genet.*, **18**, 203–210.
13. Aylsworth, A.S., Thomas, G.H., Hood, J.L., Malouf, N. and Libert, J. (1980) A severe infantile sialidosis: clinical, biochemical and microscopic features. *J. Pediatr.*, **96**, 662–668.
14. Johnson, W.G., Cohen, C.S., Miranda, A.F., Waran, S.P. and Chutorian, A.M. (1980) Alpha-locus hexosaminidase genetic compound with juvenile gangliosidosis phenotype: clinical, genetic and biochemical studies. *Am. J. Hum. Genet.*, **32**, 43A.
15. Beck, M., Bender, S.W., Reiter, H.L., Otto, W., Bassler, R., Dancygier, H. and Gehler, J. (1984) Neuraminidase deficiency presenting as non-immune hydrops fetalis. *Eur. J. Pediatr.*, **143**, 135–139.
16. Pshezhetsky, A.V., Richard, C., Michaud, L., Igdoura, S., Wang, S., Elsliger, M.A., Qu, J., Leclerc, D., Gravel, R., Dallaire, L. and Potier, M. (1996) Sialidosis: cloning, expression and chromosomal mapping of human lysosomal sialidase (neuraminidase). *Am. J. Hum. Genet.*, **59**, **4**, A279.
17. Pshezhetsky, A.V., Richard, C., Michaud, L., Igdoura, S., Wang, S., Elsliger, M.A., Qu, J., Leclerc, D., Gravel, R., Dallaire, L. and Potier, M. (1997) Cloning, expression and chromosomal mapping of human lysosomal sialidase and characterization of mutations in sialidosis. *Nature Genet.*, **15**, 316–320.
18. Bonten, E., van der Spoel, A., Fornerod, M., Grosveld, G. and d'Azzo, A. (1996) Characterization of human lysosomal neuraminidase defines the molecular basis of the metabolic storage disorder sialidosis. *Genes Dev.*, **10**, 3156–3168.
19. Milner, C.M., Smith, S.V., Carrillo, M.B., Taylor, G.L., Hollinshead, M. and Campbell R.D. (1997) Identification of a sialidase encoded in the human major histocompatibility complex. *J. Biol. Chem.*, **272**, 4549–4558.
20. Rottier, R.J., Bonten, E. and d'Azzo, A. (1998) A point mutation in the neu-1 locus causes the neuraminidase defect in the SM/J mouse. *Hum. Mol. Genet.*, **7**, 313–321.
21. Carrillo, M.B., Milner, C.N., Ball, S.T., Snock, M. and Campbell, R.D. (1997) Cloning and characterization of sialidase from the murine histocompatibility-2 complex: low levels of mRNA and a single amino acid mutation are responsible for reduced sialidase activity in mice carrying the Neu1a allele. *Glycobiology*, **7**, 975–986.

22. Igdoura, S.A., Gafuik, C., Mertineit, C., Saberi, F., Pshezhetsky, A.V., Potier, M., Trasier, J.M. and Gravel, R.A. (1998) Cloning of the cDNA and the gene encoding mouse lysosomal sialidase and correction of sialidase deficiency in human sialidosis and mouse SM/J fibroblasts. *Hum. Mol. Genet.*, **7**, 115–121.
23. Thomas, G.H., Goldberg, M.F., Miller, C.S. and Reynolds, L.W. (1979) Neuraminidase deficiency in the original patient with Goldberg Syndrome. *Clin. Genet.*, **16**, 323–330.
24. Cantz, M., Gehler, J. and Spranger, J. (1977) Mucolipidosis I: increased sialic acid content and deficiency of an α-*N*-acetylneuraminidase in cultured fibroblasts. *Biochem. Biophys. Res. Commun.*, **74**, 732–738.
25. Johnson, W.G., Thomas, G.H., Miranda, A.F., Driscoll, J.M., Wigger, J.H., Yeh, M.N., Schwartz, R.C., Cohen, C.S., Berdon, W.E. and Koenigsberger, M.R. (1980) Congenital sialidosis: Biochemical studies; clinical spectrum in four sibs; two successful prenatal diagnoses. *Am. J. Hum. Genet.*, **32**, 43A.
26. Carey, W.F., Fletcher, J.M. and Wong, M.C. (1997) A case of sialidosis with unusual results. In *Proceedings of the 7th International Congress of Inborn Errors of Metabolism*. Vienna, Austria, p. 104.
27. Tylki-Szymanska, A., Lugowska, A. and Czartoryska, B. (1996) Neuraminidase deficiency presenting as a nephrosialidosis: The first case detected in Poland. *Acta Paediatr. Jpn*, **38**, 529–532.
28. Palmeri, S., Villanova, M., Malandrini, A., van Diggelen, O., Huijmans, J., Ceuterick, C., Rufa, A., DeFalco, D., Ciacci, G., Martin, J. and Guazzi, G. (2000) Type I sialidosis: a clinical, biochemical and neuroradiological study. *Eur. Neurol.*, **43**, 88–94.
29. Orita, M., Suzuki, Y., Sekiya, T. and Hayashi, K. (1989) Rapid and sensitive detection of point mutations and DNA polymorphisms using the polymerase chain reaction. *Genomics*, **5**, 874–879.
30. Vinogradova, M.V., Michaud, L., Mezentsev, A.V., Lukong, K.E., El-Alfy, M., Morales, C.R., Potier, M. and Pshezhetsky, A.V. (1998) Molecular mechanism of lysosomal sialidase defiency in galactosialidosis involves its rapid degradation. *Biochem. J.*, **330**, 641–650.
31. Varghese, J.N., Laver, W.G. and Colman, P.M. (1983) Structure of the influenza virus glycoprotein antigen neuraminidase at 2.9 Å resolution. *Nature*, **303**, 35–40.
32. Burmeister, W.P., Ruigrok, R.W.H. and Cusack, S. (1992) The 2.2 Å resolution crystal structure of influenza B neuraminidase and its complex with sialic acid. *EMBO J.*, **11**, 49–56.
33. Crennell, S.J., Garman, E.F., Laver, W.G., Vimr, E.R. and Taylor, G. (1993) Crystal structure of a bacterial sialidase (from *Salmonela typhimurium* LT2) shows the same fold as an influenza virus neuraminidase. *Proc. Natl Acad. Sci. USA*, **90**, 9852–9856.
34. Gaskell, A., Crennell, S. and Taylor, G. (1995) The three domains of a bacterial sialidase: a β-propeller, an immunoglobulin module and a galactose-binding jelly-roll. *Structure*, **3**, 1197–1205.
35. Crennell, S.J., Garman, E.F., Laver, W.G., Vimr, E.R. and Taylor, G. (1994) Crystal structure of a *Vibrio cholerae* sialidase reveals dual lectin-like domains in addition to the catalytic domain. *Structure*, **2**, 535–544.
36. Von Itzstein, M., Wu, W.Y., Kok, G.B., Pegg, M.S., Dyason, J.C., Jin, B., Phan, T.V., Smythe, M.L., White, H.F., Oliver, S.W. *et al.* (1993) Rational design of potent sialidase-based inhibitors of influenza virus replication. *Nature*, **363**, 418–423.
37. Taylor, G. (1996) Sialidases: structures, biological significance and therapeutic potential. *Curr. Opin. Struct. Biol.*, **6**, 830–837.
38. d'Azzo, A., Hoogeveen, A., Reuser, A.J., Robinson, D. and Galjaard, H. (1982) Molecular defect in combined β-galactosidase and neuraminidase deficiency in man. *Proc. Natl Acad. Sci. USA*, **79**, 4535–4539.
39. Van der Horst, G.J., Galjart, N.J., d'Azzo, A., Galjaard, H. and Verheijen, F.W. (1989) Identification and in vitro reconstitution of lysosomal neuraminidase from human placenta. *J. Biol. Chem.*, **264**, 1317–1322.
40. Pshezhetsky, A.V. and Potier, M. (1996) Association of *N*-acetylgalactosamine-6-sulfate sulfatase with the multienzyme lysosomal complex of β-galactosidase, cathepsin A and neuraminidase. *J. Biol. Chem.*, **271**, 28359–28365.
41. Hoogeveen, A.T., Verheijen, F.W. and Galjaard, H. (1983) The relation between human lysosomal β-galactosidase and its protective protein. *J. Biol. Chem.*, **258**, 12143–12146.
42. Pshezhetsky, A.V., Elsliger, M.-A., Vinogradova, M. and Potier, M. (1995) Human lysosomal β-galactosidase–cathepsin A complex: definition of the β-galactosidase-binding interface on cathepsin A. *Biochemistry*, **34**, 2431–2440.
43. D'Agrosa, R.M., Hubbes, M., Zhang, S., Shankaran, R. and Callahan, J.W. (1992) Characterization of the β-galactosidase–carboxypeptidase complex in GM1-gangliosidosis and β-galactosialidosis fibroblasts. *Biochem. J.*, **285**, 833–838.
44. Okamura-Oho, Y., Zhang, S., Hilson, W., Hinek, A. and Callahan, J. (1996) Early proteolytic cleavage with loss of a C-terminal fragment underlies altered processing of the β-galactosidase precursor in galactosialidosis. *Biochem. J.*, **313**, 787–794.
45. van der Spoel, A., Bonten, E. and Azzo, A. (1998) Transport of human lysosomal neuraminidase to mature lysosomes requires protective protein/cathepsin A. *EMBO J.*, **17**, 1588–1597.
46. d'Azzo, A., Andria, G., Strisciuglio, P. and Galijaard, H. (1995) Galactosialidosis. In Scriver, C.R., Beaudet, A.L., Sly, W.S. and Vallee, D. (eds), *Metabolic and Molecular Bases of Inherited Disease*, Vol. 2. McGraw-Hill, New York, NY, pp. 2835–2837.
47. Rudenko, G., Bonten, E., Hol, W.G.H. and d'Azzo, A (1998) The atomic model of the human protective protein/cathepsin A suggests a structural basis for galactosialidosis. *Proc. Natl Acad. Sci. USA*, **95**, 621–615.
48. Maniatis, T., Fritsch, E.F. and Sambrook, J. (eds) (1982) *Molecular Cloning: A Laboratory Manual*. Cold Spring Harbor Laboratory Press, Cold Spring Harbor, NY.
49. Triggs-Raine, B.L., Akerman, B.R., Clarke, J.T. and Gravel, R.A. (1991) Sequence of DNA flanking the exons of the HEXA gene and identification of mutations in Tay–Sachs disease. *Am. J. Hum. Genet.*, **49**, 1041–1054.
50. Okada, S. and O'Brien, J.S. (1968) Generalized gangliosidosis: β-galactosidase deficiency. *Science*, **160**, 1002–1004.
51. Potier, M., Mameli, L., Belisle, M., Dallaire, L. and Melançon, S.B. (1979) Fluorometric assay of neuraminidase with a sodium (4-methylumbelliferyl-α-D-*N*-acetylneuraminate) substrate. *Anal. Biochem.*, **94**, 287–296.
52. Rome, L.H., Garvin, A.J., Allietta, M.M. and Neufeld, E.F. (1979) Two species of lysosomal organelles in cultured human fibroblasts. *Cell*, **17**, 143–153.
53. Pshezhetsky, A.V., Vinogradova, M.V., Elsliger, M.-A., El-Zein, F., Svedas, V.K. and Potier, M. (1995) Continuous spectrophotometric assay of human lysosomal cathepsin A/protective protein in normal and galactosialidosis cells. *Anal. Biochem.*, **230**, 303–307.
54. Bradford, M.M. (1976) A rapid and sensitive method for the quantitation of microgram quantities of protein utilizing the principle of protein–dye binding. *Anal. Biochem.*, **72**, 248–254.
55. Laemmli, U.K. (1970) Cleavage of structural proteins during the assembly of the head of bacteriophage T4. *Nature*, **227**, 680–685.